A broadband solar absorber with 12 nm thick ultrathin a-Si layer by using random metallic nanomeshes

Tianyi Sun, Chuan Fei Guo, Feng Cao, Eser Metin Akinoglu, Yang Wang, Michael Giersig, Zhifeng Ren, and Krzysztof Kempa

Articles you may be interested in

Hybrid ZnO nanowire/a-Si:H thin-film radial junction solar cells using nanoparticle front contacts
Appl. Phys. Lett. **107**, 143903 (2015); 10.1063/1.4932649

Cascading metallic gratings for broadband absorption enhancement in ultrathin plasmonic solar cells
Appl. Phys. Lett. **104**, 151106 (2014); 10.1063/1.4871584

Plasmonic metal nanocubes for broadband light absorption enhancement in thin-film a-Si solar cells
J. Appl. Phys. **115**, 124317 (2014); 10.1063/1.4869785

Application of SixNy:Hz (SiN) as index matching layer in a-Si:H thin film solar cells
J. Renewable Sustainable Energy **5**, 031605 (2013); 10.1063/1.4807609

Thickness determination of very thin amorphous and microcrystalline silicon layers using reflection/transmission measurements
Appl. Phys. Lett. **85**, 5096 (2004); 10.1063/1.1825063

A broadband solar absorber with 12 nm thick ultrathin *a*-Si layer by using random metallic nanomeshes

Tianyi Sun,[1,2,a)] Chuan Fei Guo,[1,a)] Feng Cao,[1] Eser Metin Akinoglu,[3] Yang Wang,[4] Michael Giersig,[3,5] Zhifeng Ren,[1,b)] and Krzysztof Kempa[2,b)]

[1]*Department of Physics and TcSUH, University of Houston, Houston, Texas 77204, USA*
[2]*Department of Physics, Boston College, Chestnut Hill, Massachusetts 02467, USA*
[3]*Department of Physics, Freie Universität Berlin, 14195 Berlin, Germany*
[4]*Institute for Advanced Materials (IAM), South China Academy of Advanced Optoelectronics,*
South China Normal University, Guangzhou 510006, China
[5]*Department of Chemistry, Adam Mickiewicz University (UAM), Poznan, Poland*

We show in theory, simulations, and experiments that, by applying random metallic nanomeshes, a broad-band multilayered structure with a 12 nm thick *a*-Si film as the active layer can absorb 89% of the total solar energy in the visible range from 400 nm to 700 nm. Such broadness and high absorption can be attributed to the random scattering introduced by the aperiodic metallic nanomeshes and the plasmonic-metamaterial design. The broadband and smooth electromagnetic response, combined with a very high absorption, is desired for solar energy harvesting devices, making this structure a good candidate for high efficiency photovoltaics with ultra-thin active layers. © 2014 AIP Publishing LLC. [http://dx.doi.org/10.1063/1.4884936]

Since the discovery of the extraordinary optical transmission,[1] the electromagnetic response of periodic arrays of sub-wavelength holes in metal films and metallic wire networks have been intensively studied in recent years in the fields of plasmonics and metamaterials.[2–5] A periodic array of holes in a metallic film allows the external radiation to couple to the surface plasmon polaritons (SPP), charge density waves propagating along the film. Metal wire-mesh systems, which are widely used as conducting transparent electrodes and wavelength-selective filters in different frequency ranges,[6–9] can be viewed also as such hole-perforated metal films. As expected, the array periodicity and the geometry of holes in these structures play an important role in determining their optical properties.[10] In the scenario of solar energy harvesting, there have been multiple pioneering researches to take advantage of the metallic wire systems by integrating them into thin film solar cells.[11–13] However, due to the complexity of fabricating subwavelength periodic structures, the high cost of these designs has become a main barrier towards commercialization in mass production. In this paper, we show that, by removing the in-plane long-range order in a metallic nanomesh and by randomization of the hole shapes, the generated plasmonic, plasmon polaritonic, or photonic modes can de-tune and/or de-cohere, leading to a smooth, broad-band response. Such random metallic nanostructures can be fabricated in a large scale with low cost and directly integrated into an ultrathin plasmonic-metamaterial absorber scheme. The plasmonic-metamaterial absorber structure with only 12 nm thick ultrathin active *a*-Si layer proves to exhibit a high absorption of 89% in the total solar energy in the visible range (400–700 nm).

In periodic arrays (e.g., holes in a metallic film or polarizable point-dipoles), plasmonic, polaritonic, or pure photonic modes can propagate unscattered as a result of the Bloch theorem, unless the Bragg diffraction prevents their propagation at the Brillouin zone in the k-space, leading to gaps in their spectrum (band structure).[14,15] Gaps can be generated also without the help of the Bragg diffraction, by polaritonic coupling of photons to polarizable charges, which opens a large gap in the photonic (polaritonic) spectrum of bulk metals below the plasma frequency.[15,16] In this polaritonic (or photonic) crystal picture, the spectral response of the array (e.g., transmission), characterized by multiple maxima and minima, corresponds to bands and gaps in the polaritonic (or photonic) spectrum.[14,15] In a random array, the broken translational symmetry leads to scattering of the modes as well as to mode localization.[17–20] The situation is analogous to the electronics of crystals transforming into amorphous solids: gradual deterioration of the long-range order leads to gradual formation of tails of localized states, extending from the bands into the gaps. The resulting electronic spectrum transforms from gapped into gapless. A similar situation happens to plasmonic/photonic crystals gradually losing the long-range order[20] and results in the spectral response becoming increasingly smooth.

To demonstrate this, we compare the optical response of a periodic (hexagonal) array of circular holes in a gold film with a random gold nanomesh. Both structures have the same metal fill factor of 30% (fraction of the surface covered by metal). The periodic structure was made in a gold film of 50 nm thickness on a sapphire substrate using the nanosphere lithography,[21,22] with the center-to-center nearest neighbor hole distance of 756 nm and the hole diameter of 663 nm. The scanning electron microscopy (SEM) micrograph of the film is shown in Fig. 1(a). To generate the random nanomesh, we employed the grain boundary lithography.[23,24] 65 nm thick SiO_2 and 100 nm thick In films were first deposited by magnetron sputtering (ORION-8, AJA international sputtering system) on a Si wafer and then etched in 20 wt. %

[a)]T. Sun and C. F. Guo contributed equally to this work.
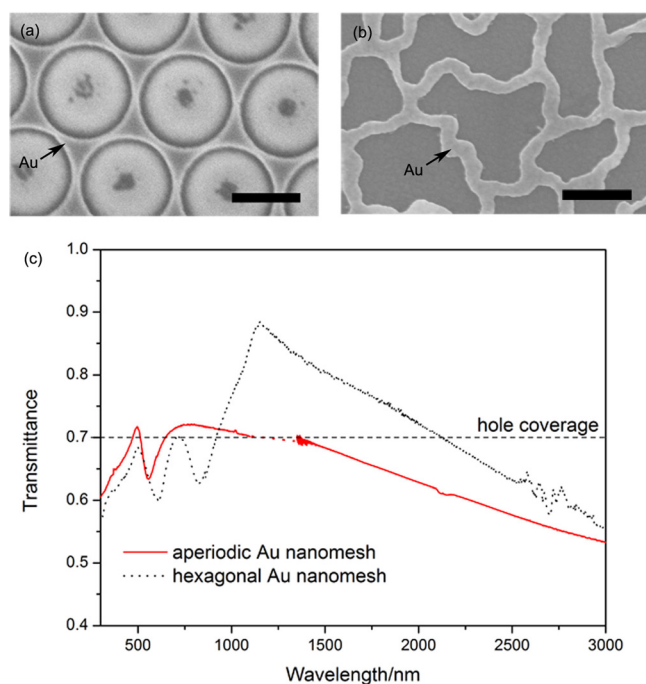[b)]Electronic addresses: kempa@bc.edu and zren@uh.edu

FIG. 1. (a) and (b) are SEM micrographs of the periodic (hexagonal) and aperiodic Au nanomeshes with the same metal coverage. Scale bars are 500 nm. (c) Transmittance of the periodic (black dotted line) and aperiodic (red solid line) Au nanomeshes.
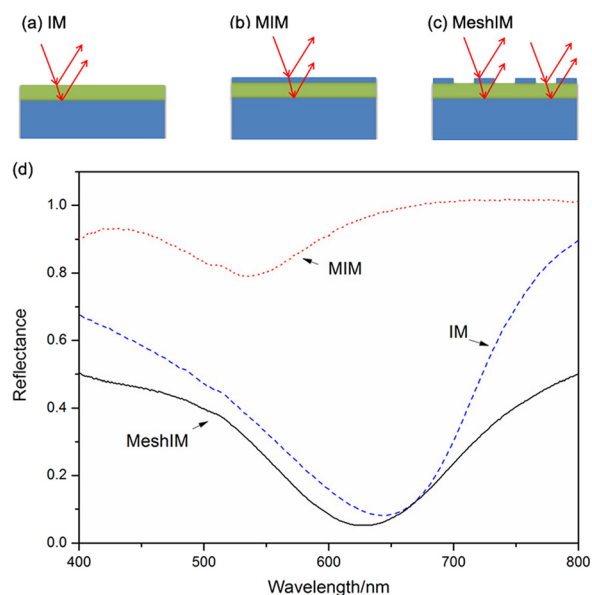

FIG. 2. Schematic side views of three multilayer structures: (a) insulator/metal (IM), (b) metal/insulator/metal (MIM), and (c) aperiodic metallic mesh/insulator/metal (MeshIM). (d) Reflectance spectra of the three structures in the visible range. Blue dashed line: 20 nm a-Si/200 nm Ag; red dotted line: 35 nm Ag/20 nm a-Si/200 nm Ag; black solid line: 35 nm aperiodic Ag mesh/20 nm a-Si/200 nm Ag.

HNO$_3$ for gap formation. The wafer was then thermal oxidized at 400 °C for 2 h to form In$_2$O$_3$ islands and rinsed in 5 wt. % HF for 12 s, leading to the formation of undercuts. The random nanomesh is formed in the gaps between In$_2$O$_3$ islands after deposition of 35 nm thick Au by e-beam evaporation. HF was introduced to dissolve the SiO$_2$ and removal of In$_2$O$_3$ islands, leaving a continuous random Au nanomesh on the flat silicon surface. The nanomesh was then transferred to a CaF$_2$ substrate using wedging transfer.[25] The SEM micrograph of the nanomesh is shown in Fig. 1(b). The metallic coverage was determined to be 31%, by statistically averaging over a large SEM micrograph. The transmittance spectra of the periodic structure, shown as a black dotted line in Fig. 1(c), were obtained at normal incidence with a Perkin Elmer 950 spectrometer. The corresponding transmittance (T) spectrum of the random structure is shown in Fig. 1(c) as a red solid line, obtained at normal incidence with Hitachi U2001 spectrometer in the wavelength range of 400 nm–1100 nm and with Thermo Scientific iS590 in the infrared (IR) range. Both spectra have been substrate normalized. The transmission results fully confirm the analysis in the previous paragraph.

It is clear that the spectrum of the random structure has fewer spectral features than the one of the periodic array. In fact, only one feature can be observed on the random array spectrum at about 520 nm. This is a universal spectral feature occurring in nanoscopic structures made of gold. It is not present in a uniform gold film, since the inter-band absorption (d-p), which occurs in the wavelength range of 250–400 nm, creates the corresponding broad-band reduction of transmittance below ~500 nm, not a narrow minimum at 600 nm.[26] Instead, this sharp feature is due to a plasmon mode excited at sufficiently small nanoscopic geometrical

features of the structures, which provides large momentum transfer during the photon-electron scattering. For example, such Mie resonance occurs commonly in sufficiently small (<50 nm) gold nanoparticles,[27–30] and it can be viewed as a Fabry-Perot like resonance of standing surface plasmon waves.[31,32] At large momentum transfers, the surface plasmons are almost not dispersing, with the corresponding frequencies approaching the surface plasmon frequency,[31,32] for gold corresponding to the wavelength $\lambda_{sp} \sim 600$ nm.[33] This feature occurs also in our periodic and random structures, since both contain large number of small geometrical confinements/constrictions of the order of 50 nm: narrow necks between quasi-triangles in Fig. 1(a) and narrow wires in Fig. 1(b). The additional features in the spectrum of the periodic sample have been explained in detail elsewhere[22] and are due to surface plasmon polaritons excited by grating effect of the periodic arrangement of holes.[1] This mechanism does not apply to the random nanomeshes, and thus allows for the smooth, feature-less nature of the spectrum. Both arrays are quite transparent (~70%), and the differences in the transmittances are due to slightly different fill factors and metal thicknesses.

Although random nanomeshes have a rather large metallic coverage (~30% in Fig. 1(b)), they are surprisingly effective in scattering forward, rather than selectively reflecting backwards when integrated to thin film structures such as insulator-metal (IM) layers with a-Si. One example of the mentioned IM structure consists of 20 nm amorphous silicon (a-Si) on a 200 nm thick Ag substrate as the back reflector, deposited by magnetron sputtering. The structure is schematically shown in Fig. 2(a). The dashed blue line in Fig. 2(d) shows the correspondent reflectance (R) spectrum as measured by the Hitachi U2001 spectrometer: a pronounced deep minimum (<10%) at about 650 nm, caused by a nontrivial phase difference between reflected light from the air/
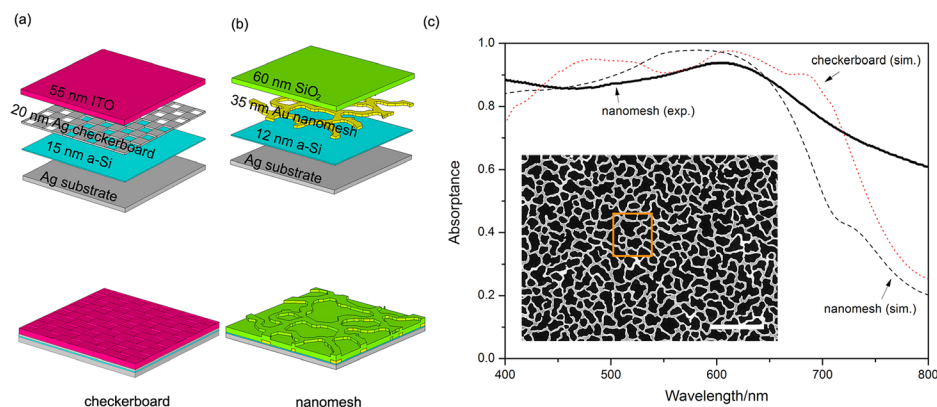
FIG. 3. Schematic views of broadband absorbers based on (a) a checkerboard structure and (b) aperiodic nanomesh. (c) Absorptance of structures in the visible range: red dotted line—checkerboard simulation; black solid line—nanomesh experiment; black dashed line—nanomesh simulation. SEM micrograph of the Au nanomesh in (b) can be found in the inset. The scale bar in the inset of (c) is 2.5 μm.

a-Si interface and the *a*-Si/Ag interface, as reported in Refs. 34 and 35. In optoelectronic applications, such structures are often accompanied with a transparent conductive electrode placed on top of the semiconductor layer. If a continuous 35 nm thick Ag layer is sputtered on the IM sample, a metal-IM (MIM) structure is formed, schematically shown in Fig. 2(b). Usually, a MIM structure forms a Fabry-Perot cavity, which is often featured by sharp resonances and used as selective filters.[33] But due to the low transmittance of the 35 nm Ag film and high absorption of *a*-Si in the visible range, the corresponding reflectance spectrum, shown as a red dotted line in Fig. 2(d), shows almost eliminated F-P action: except for a very shallow, shifted minimum at ∼550 nm, the reflectance in the whole range is above 90%. As depicted in Fig. 1(b), the random Ag nanomeshes cover a non-negligible 30% of the whole area and have a thickness of non-negligible 35 nm. If the nanomeshes of the same thickness (35 nm) are placed on the IM structure (MeshIM structure, in Fig. 2(c)) by employing the wedging transfer technique, from the spectra of IM and MIM structures, a quick guess of the MeshIM reflectance would be around 40% in the visible range. However, the measured reflectance spectrum (the black solid line in Fig. 2(d)) turns out to exhibit a slightly shifted but even broader and more pronounced minimum than that of the IM structure. This seemingly contradictive result comes from the broadness and featurelessness of the random nanomeshes. Though lying out of the subwavelength limit for the Maxwell-Garnett effective medium theory,[33] the random Ag nanomeshes and the underlying *a*-Si film can be viewed as a single layer of an effective medium, as suggested in Ref 35. In this picture, the optical response of the MeshIM structure can be seen as an effective IM structure, with the "effective *a*-Si" as the insulator that governs.

Based on the above discussion, a broad-band metamaterial superabsorber could be made using random metallic nanomeshes, inspired by the structure based on a checkerboard island pattern, whose schematic layout is shown in Fig. 3(a). This structure has been recently proposed as a basis for a class of ultra-thin solar cells, and demonstrated by simulations, requiring a featureless, flat spectral response of the front electrode.[35,36] Since the random nanomeshes offer a similar response, they have the potential to work as a replacement of the checkerboard pattern. As proof of concept for this hypothesis, we have sputtered a 12 nm *a*-Si film on a

silver coated (200 nm) silicon wafer substrate, followed by the deposition of a 35 nm thick random Au nanomesh, and 60 nm thick SiO₂ film. The layout of the structure is shown in Fig. 3(b). The structure was prepared using the same techniques mentioned above. The SEM micrograph of this structure before SiO₂ deposition is shown in the inset of Fig. 3(c). Since the structure is non-transparent, the absorbance (*A*) is given by $A = 1 - R$ and is shown in Fig. 3(c) as a black solid line. As expected, the absorbance is broad-band and large, with over 85% in the entire visible domain where the *a*-Si interband transitions are most pronounced. In comparison to the simulated absorbance of the checkerboard island pattern structure of Ref. 35, shown in Fig. 3(c) as a red dashed line, the absorbance is only slightly smaller, but just as broad as in the considered range. Finally, we perform the simulations of our nanomesh structure by employing the CST Microwave Studio software package, based on the finite difference time domain (FDTD) method. The random nanomesh pattern in the simulation was modeled directly from a 1500 nm × 1500 nm section of the SEM micrograph, marked by an orange rectangle in the inset of Fig. 3(c). Dielectric functions for all materials were taken directly from experimental data.[37] The simulation result is shown as a black dashed line in Fig. 3(c), in good agreement with the corresponding experimental results in the wavelength range of 400–650 nm. For wavelengths above 650 nm, the experimental absorbance is larger than the simulated one. This discrepancy is due to an insufficient absorption in the modeled dielectric functions of the metal and possibly *a*-Si. We point out that this parameter can vary and depends strongly on a specific deposition technique, as illustrated by differences in the experimental results of Refs. 26 and 37.

To estimate the potential for photovoltaic applications, we have calculated energy absorption partitions in individual layers of the nanomesh structure, shown as the four lines in Fig. 4. As can be seen from the blue solid line with circles, more than 70% of the energy goes into the 12 nm thick *a*-Si layer at the maximum around 500 nm. Under solar illuminance of AM1.5 on the earth surface, this spectrum means 57% of the total solar energy from 400 nm to 700 nm is absorbed by the *a*-Si layer. As the wavelength increases towards the bandgap of *a*-Si around 700 nm, the imaginary part of the permittivity decreases fast and thus the energy absorbed in *a*-Si was overtaken by Au nanomeshes. The energy dissipation in metallic parts is not favored for solar
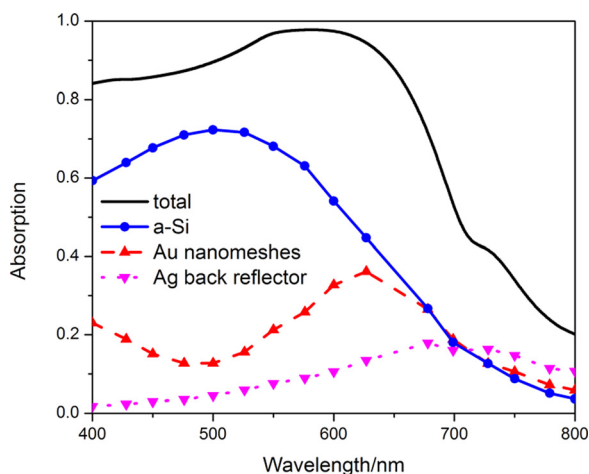
FIG. 4. Energy distribution of absorbed solar energy in individual layers: total (black solid line), a-Si (blue solid line with circles), Au nanomeshes (red dashed line with triangles), and Ag back reflector (pink dotted line with reverse triangles).

cells. Preliminary simulation indicates this problem can be solved by replacing *a*-Si with other photovoltaic materials with a smaller bandgap, such as *c*-Si and Ge, where absorption in nanomeshes is much less.

Compared with $250 \sim 300$ nm thick *a*-Si used in common *a*-Si solar cells, the nanomesh structure achieves high absorption with much less material (12 nm vs. 300 nm, only 1/25th). As an estimate, with existing reported conversion efficiency of 2.5% for 20 nm thick *a*-Si solar cell and 10.1% for the best conventional *a*-Si solar cells,[38,39] the same amount of *a*-Si could be used to generate 5 times more electricity in such ultrathin cells than in common cells. In addition, the connecting metallic nanomesh is proven to be very conducting, with sheet resistance less than 10 $\Omega/\square$. This creates the possibility of reducing fabrication costs by removing the expensive ITO and the full structure such as Fig. 3(b) can work as a promising platform for a new generation of soft and flexible solar cells.[40]

In conclusion, we have demonstrated that a metallic random nanomesh has a broad-band and smooth electromagnetic response and very high transparency, compared with a periodic structure. Use of the nanomeshes enables a broad-band solar absorber platform with only 12 nm thick *a*-Si as the active layer. The 89% absorption of total solar energy in the visible range makes such structures an excellent candidate for solar energy harvesting.

[1]T. W. Ebbesen, H. J. Lezec, H. F. Ghaemi, T. Thio, and P. A. Wolff, Nature **391**, 667–669 (1998).
[2]A. Mitsuishi, Y. Otsuka, S. Fujita, and H. Yoshinaga, Jpn. J. Appl. Phys., Part 1 **2**, 574 (1963).
[3]F. Yang and J. R. Sambles, Phys. Rev. Lett. **89**, 063901 (2002).
[4]J. Prikulis, P. Hanarp, L. Olofsson, D. Sutherland, and M. Käll, Nano Lett. **4**, 1003 (2004).
[5]S. Zhang, W. Fan, K. J. Malloy, S. R. J. Brueck, N. C. Panoiu, and R. M. Osgood, Opt. Express **13**, 4922 (2005).
[6]G. Ctistis, P. Patoka, X. Wang, K. Kempa, and M. Giersig, Nano Lett. **7**, 2926 (2007).
[7]F. Keilmann, Int. J. Infrared Millimeter Waves **2**, 259 (1981).
[8]R. Ulrich, Infrared Phys. **7**, 37 (1967).
[9]C. M. Rhoads, E. K. Damon, and B. A. Munk, Appl. Opt. **21**, 2814 (1982).
[10]K. J. K. Koerkamp, S. Enoch, F. B. Segerink, N. F. van Hulst, and L. Kuipers, Phys. Rev. Lett. **92**, 183901 (2004).
[11]V. Ferry, M. Verschuuren, M. van Lare, R. Schropp, H. Atwater, and A. Polman, Nano Lett. **11**, 4239 (2011).
[12]H. Atwater and A. Polman, Nature Mater. **9**, 205 (2010).
[13]M. Green and S. Pillai, Nat. Photonics **6**, 130 (2012).
[14]J. D. Joannopoulos, R. D. Meade, and J. N. Winn, *Photonic Crystals: Molding the Flow of Light* (Princeton University Press, New York, 1995).
[15]K. Kempa, R. Ruppin, and J. B. Pendry, Phys. Rev. B **72**, 205103 (2005).
[16]X. Wang and K. Kempa, Phys. Rev. B **71**, 233101 (2005).
[17]S. John, Phys. Rev. Lett. **53**, 2169 (1984).
[18]M. I. Stockmann, S. V. Faleev, and D. J. Bergman, Phys. Rev. Lett. **87**, 167401 (2001).
[19]K. Seal, D. A. Genov, A. K. Sarychev, H. Noh, V. M. Shalaev, Z. C. Ying, X. Zhang, and H. Cao, Phys. Rev. Lett. **97**, 206103 (2006).
[20]X. Wang, K. Kempa, Z. Ren, and B. Kimball, Appl. Phys. Lett. **84**, 1817 (2004).
[21]E. Akinoglu, T. Sun, J. Gao, M. Giersig, Z. Ren, and K. Kempa, Appl. Phys. Lett. **103**, 171106 (2013).
[22]T. Sun, E. M. Akinoglu, C. Guo, T. Paudel, J. Gao, Y. Wang, M. Giersig, Z. F. Ren, and K. Kempa, Appl. Phys. Lett. **102**, 101114 (2013).
[23]C. F. Guo, T. Sun, Y. Wang, J. Gao, Q. Liu, K. Kempa, and Z. Ren, Small **9**, 2415 (2013).
[24]C. F. Guo, T. Sun, Q. Liu, Z. Suo, and Z. Ren, Nat. Commun. **5**, 3121 (2014).
[25]G. F. Schneider, V. E. Calado, H. Zandbergen, L. M. K. Vandersypen, and C. Dekker, Nano Lett. **10**, 1912 (2010).
[26]P. B. Johnson and R. W. Christy, Phys. Rev. B **6**, 4370 (1972).
[27]G. Mie, Ann. Phys. **330**, 377 (1908).
[28]W. Ekardt, Phys. Rev. B **31**, 6360 (1985).
[29]J. Nelayah, L. Gu, W. Sigle, C. T. Koch, I. Pastoriza-Santos, L. M. Liz-Marzán, and P. A. van Aken, Opt. Lett. **34**, 1003 (2009).
[30]L. B. Scaffardi and J. O. Tocho, Nanotechnology **17**, 1309 (2006).
[31]K. Kolwas, Appl. Phys. B **66**, 467 (1998).
[32]Y. Peng, C. Marcoux, P. Patoka, M. Hilgendorff, M. Giersig, and K. Kempa, Appl. Phys. Lett. **96**, 133104 (2010).
[33]O. S. Heavens, *Optical Properties of Thin Solid Films* (Dover Publications, Inc., New York, 1991).
[34]M. A. Kats, R. Blanchard, P. Genevet, and F. Capasso, Nature Mater. **12**, 20 (2012).
[35]Y. Wang, T. Sun, T. Paudel, Y. Zhang, Z. Ren, and K. Kempa, Nano Lett. **12**, 440 (2012).
[36]K. Kempa, Phys. Status Solidi RRL **4**, 218 (2010).
[37]D. Palik, *Handbook of Optical Constants of Solids* (Academic Press, Boston, 1985).
[38]K. Kempa, M. Naughton, Z. Ren, A. Herczynski, T. Kirkpatrick, J. Rybczynski, and Y. Gao, Appl. Phys. Lett. **95**, 233121 (2009).
[39]M. Green, K. Emery, Y. Hishikawa, W. Warta, and E. Dunlop, Prog. Photovoltaics Res. Appl. **22**, 1 (2014).
[40]C. F. Guo, T. Sun, F. Cao, Q. Liu, and Z. Ren, Light Sci. Appl. **3**, e161 (2014).